Global J. Environ. Sci. Manage. 10(4): 1675-1686, Autumn 2024, Serial #40

Global Journal of Environmental Science and Management
(GJESM)

Homepage: https://www.gjesm.net/

Podcasts

ORIGINAL RESEARCH PAPER

Application of iron-rich slag to capture carbon dioxide gas through direct gas-solid carbonation

F. Abdul[1,*], R.F. Rahman[1], K.A. Purwanto[1], F.I. Ma'ruf[1], Y. Setiyorini[1], V.A. Setyowati[2], S. Pintowantoro[1]

[1] *Department of Materials and Metallurgical Engineering, Faculty of Industrial Technology and System Engineering, Institut Teknologi Sepuluh Nopember, Surabaya, 60111, Indonesia*

[2] *Department of Mechanical Engineering, Faculty of Industrial Technology, Institut Teknologi Adhi Tama Surabaya, Surabaya, 60117, Indonesia*

ARTICLE INFO

Article History:
Received 23 December 2023
Revised 28 February 2024
Accepted 03 April 2024

Keywords:
Carbon dioxide (CO_2)
Iron oxide carbonation
Sequestration
Sustainable process
Waste utilization

ABSTRACT

BACKGROUND AND OBJECTIVES: The nickel processing industry has always been related with the issue of carbón dioxide emission. The production of carbon dioxide occurs at different phases of nickel processing, from pretreatment to smelting and refining. In addition to offgas, the nickel processing sector also produces solid waste known as slag, which is a byproduct of both smelting and refining processes. One of the slags in the nickel industry is known to contain iron, which is dominant compared to other elements. The primary objective of this study is to investigate the process of carbon dioxide capture by utilizing iron-rich slag derived from the nickel processing industry. The aim is to assess the feasibility of applying iron-rich slag from nickel smelters in the solid carbonation gas process for carbon dioxide capture, focusing on chemical reactions and overall kinetics.

METHODS: The iron-rich slag analyzed in this study contains a significant amount of iron oxide. It is theoretically anticipated that the iron oxide content in iron-rich slag could potentially sequester carbon dioxide. The study commenced by preparing the materials, undergoing the carbonation process, and then conducting various characterizations including X-ray diffractometer analysis and thermal gravimetric analysis. Additionally, calculations were performed to determine the percentage of carbon dioxide in the sample and the efficiency of carbonation. The kinetics analysis was also carried out using several models, such as mass transport, chemical reaction, and diffusion-controlled model to estimate the carbón dioxide capture mechanism that occurs.

FINDINGS: The carbon dioxide capture capacity of the iron-rich slag from the ferronickel industry is somewhat limited, albeit still relatively modest. Iron-rich slag was effectively utilized to capture carbon dioxide after thorough analysis. After undergoing a carbonation process for a duration of 4 hours, the percentage of carbon dioxide in the slag witnessed a significant increase, rising from an initial value of 0.28 percent to 1.12 percent. The capture of carbón dioxide gas is due to the reaction between silicate with carbón dioxide gas and water vapor to form siderite. The iron-rich slag operates under the diffusion-controlled model when it comes to capturing carbon dioxide.

CONCLUSION: Iron-rich slag is reported to capture carbón dioxide at 175 degrees celsius with carbón dioxide and water vapor condition, which is proven both from thermodynamic calculations and experiments. Iron(II) carbonate is a carbonate compound generated by the carbón dioxide capture reaction by iron-rich slag. However, the stability of iron(II) carbonate in carbón dioxide and water vapor atmosphere is something that needs to be considered in future research. Further investigation can be conducted in the future to explore the potential of utilizing iron-rich slag for capturing carbon dioxide gas, building upon the findings of this preliminary study.

DOI: 10.22034/gjesm.2024.04.11

This is an open access article under the CC BY license (http://creativecommons.org/licenses/by/4.0/).

NUMBER OF REFERENCES	NUMBER OF FIGURES	NUMBER OF TABLES
45	7	2

*Corresponding Author:
Email: *fakhreza.abdul@mat-eng.its.ac.id*
Phone: +300 561 6226
ORCID: 0000-0003-1048-0717

Note: Discussion period for this manuscript open until October 1, 2024 on GJESM website at the "Show Article".

INTRODUCTION

Carbon dioxide (CO_2) is one of the greenhouse gases that contribute to climate change (Hassan, *et al.*, 2021). The nickel/ferronickel industry, like many others in the industrial sector, contributes to the emission of CO_2 into the atmosphere. The nickel/ferronickel smelter industry is one of the industries that produces high CO_2 emissions. The emission of CO_2 varies significantly based on the type of nickel smelter process and technology utilized. For instance, a nickel smelter utilizing Blast Furnace technology to manufacture nickel pig iron (NPI) will release 7 tons of CO_2 for every ton of NPI produced. On the other hand, a nickel smelter that uses the rotary kiln-electric furnace (RK-EF) technology will produce 6 tonnes of CO_2 per tonne of ferronickel product (Wei *et al.*, 2020). In the processing of ferronickel from lateritic ore, the primary extraction stage is responsible for the majority of CO_2 emissions, accounting for approximately 65%. On the other hand, stages like mining and ore preparation contribute only 35% to the overall emissions (Mistry *et al.*, 2016). In comparison to iron and steel smelters, the emission of CO_2 from iron smelters amounts to approximately 1.89 tonnes per tonne of crude steel produced (World Steel Association, 2021). This shows that the nickel smelter industry produces a significant amount of CO_2 gas. This could be caused by several factors. First, mineralogically, nickel ore contains small nickel and moderate iron content. In nature, nickel ores contain only about 1.25 percent (%) nickel (Ni) (Widyartha *et al.*, 2020; Pintowantoro *et al.*, 2021). The conversion of iron in nickel ore to metallic iron is not entirely complete. Moreover, the presence of numerous impurities in nickel ore, along with the elevated melting temperature of the impure compound, contributes to a higher specific energy demand for the production of ferronickel in comparison to steel. To produce 1 tonne of ferronickel, it is estimated that 110 giga joule (GJ) of energy is required (Wei *et al.*, 2020). Conversely, the production of 1 tonne of steel requires approximately 20 GJ of energy (Sun *et al.*, 2020; Sun *et al.*, 2022). Moreover, in contrast to the iron and steel industry which spends a lot of research and massive programs to reduce CO_2 emissions, such as CO_2 Ultimate reduction system for cool earth 50 (COURSE50), Ultra-low CO_2 steelmaking (ULCOS), Hydrogen breakthrough ironmaking technology (HYBRIT), American iron and steel Institute (AISI) program, and SAlzgitter Low CO_2 Steelmaking (SALCOS) (Liu *et al.*, 2021), the nickel smelter industry is relatively less aggressive implementing programs to decrease its CO_2 gas emissions. It is also possible to reduce CO_2 gas production in the nickel smelter industry by capturing CO_2 gas or through carbon capture and storage (CCS) technology. CCS itself is an effective technology in reducing the release of CO_2 into the atmosphere (Liu *et al.*, 2022). It would be even better if the CO_2 gas capture product could be reused. Thus, the idea of mineral carbon capture and utilization (MCC and U) technology emerged (Iizuka *et al.*, 2017; Ho *et al.*, 2020). Mineral carbonation involves the utilization of oxide compounds that have the ability to react with CO_2, resulting in the formation of carbonated products. Various raw materials, such as steel slag, can be employed for mineral carbonation (Chen *et al.*, 2021), fly ash (Ho *et al.*, 2021a), concrete waste (Ho *et al.*, 2021b), etc. This MCC and U technology is a suitable technology for centralized and localized application in every industry that releases CO_2 gas, including the nickel smelter industry. The slag from nickel smelting is recognized for its composition of alkaline earth metal compounds, including magnesium oxide (MgO) and calcium oxide (CaO) present in silicate or alumino silicate forms. This means that nickel smelter slag has the potential to be utilized as a material in the MCC and U process. Nickel slag generally contains 0.50-2.40% CaO and 30.58 – 31.11% MgO as well as other compounds such as silicon dioxide (SiO_2), ferrous oxde (FeO), aluminium oxide (Al_2O_3), etc. (Nuruzzaman *et al.*, 2022; Kuri *et al.*, 2022; Wu *et al.*, 2022). So that nickel slag has a theoretical CO_2 capture capability of around 29.63-33.95% (Abdul, *et al.*, 2023; Kuri *et al.*, 2021; Li *et al.*, 2022; Tang *et al.*, 2022). Mineralogically, ferronickel slag has dominant minerals of forsterite (Gao *et al.*, 2021), olivine (Shang *et al.*, 2021), and clinoenstatite (Zulhan *et al.*, 2021). Nevertheless, it should be acknowledged that there are specific byproducts originating from the nickel sector that exhibit a significant concentration of iron, while containing minimal quantities of magnesium and calcium. This type of slag is likely to be obtained at the converting stage (Wang *et al.*, 2018; Kasikov *et al.*, 2022). The direct gas-solid carbonation method is reported to be applicable for CO_2 capture using industrial waste. Fly ash has the potential to be utilized in the gas-solid carbonation process under conditions of 600 °C and

1 bar pressure (Liu *et al.,* 2018). According to reports, the direct gas-solid carbonation technique was employed to utilize steelmaking slag for CO_2 capture. This process was conducted at ambient temperature and under 10 bar pressure, resulting in a carbonation efficiency of 3.7% (Revathy *et al.,* 2016). The capture of CO_2 by Redmud has been documented through direct gas-solid carbonation. Remarkably, it achieves a carbonation efficiency value of 9.9% under specific operating conditions, including a temperature of 60 °C, a pressure of 45 bar, and the utilization of pure CO_2 (Revathy *et al.,* 2021). Thus, Fe-rich slag obtained from nickel smelter is not only a waste that is thrown away but can also be used to reduce CO_2 gas produced by the nickel smelter industry. Slag from the ferronickel industry has also been reported to affect the health of nearby residents. Some diseases, such as rhinitis, pruritus, and dermatitis, are reported to increase with the operation of the ferronickel industry (Han and Hong, 2018). The aim of this study is to investigate the absorption of CO_2 by Fe-rich slag derived from nickel smelting, with a focus on the lack of existing literature on this topic. Furthermore, a preliminary examination will be carried out to assess the potential of iron-rich nickel smelting slag as a viable material for CO_2 absorption through the semi-dry carbonate method. Utilizing slag can also reduce the amount of slag dumped on the land. This study (experiment and its analysis) was conducted in 2022-2023 in Indonesia.

MATERIALS AND METHODS

Materials

This study uses slag obtained from a nickel processing industry in Indonesia. Table 1 shows the slag composition used in the current study based on X-ray fluroscence (XRF). Based on Table 1, it appears that nickel slag has a high FeO content, reaching 75.25%. The slag has a low CaO content, which is only 0.14% and no MgO. Thus, the carbonation process that occurs will be only influenced by the content of FeO.

Judging from its content, it appears that the nickel slag in this study is not the primary slag generated during the smelting procedure. Typically, nickel slag is known to have elevated levels of Mg and Si, as indicated in previous studies (Pintowantoro *et al.,* 2022; Abdul *et al.*, 2023; Abdul *et al.,* 2024). The nickel slag in this study is believed to originate from the refining or converting stage following the smelting of ferronickel. Based on its chemical content, the element that may bind CO_2 is iron oxide given the very low Ca content in the slag. In this study, to simplify the analysis, all SiO_2 is assumed to bind with FeO in the form of fayalite (Fe_2SiO_4). Hence, approximately 27% of the FeO present in the slag is in the form of oxide, while the remaining 73% is Fe2SiO4. Considering the FeO content and the existing CO_2 value in the slag prior to carbonation, the maximum possible CO_2 content in the slag is 31.27%. Given that iron is the prevailing mineral in this nickel slag, the term Fe-rich slag is employed in this study for subsequent analysis. High purity N_2 and CO_2 gas used in this study are high purity gases with a minimum purity of 99% obtained from Karina gas, Surabaya, Indonesia. In order to create water vapor, demineralized water obtained from Bratachem in Surabaya, Indonesia was utilized

Methods

The Fe-rich slag obtained was then taken at random and then crushed and sieved to pass the size of 50 standard mesh. The Fe-rich slag underwent a drying process in an oven for a duration of 3 hours under a nitrogen (N2) atmosphere. Subsequently, the dried slag was subjected to characterization using XRF and X-ray diffractometer (XRD). Following this, each dried slag sample was weighed, with a weight of 15 grams. Finally, the slag was transferred to a porcelain dish without a lid and placed back into the oven for further processing. Before initiating the carbonation process with CO_2 gas flow, the oven underwent a 3-hour N_2 feeding period for purging purposes. The flow rate for CO_2 and N_2 gases was set at 1 and 4 liters/minute, respectively. Subsequently, demineralized water was consistently introduced into the container within the furnace to avoid any water shortages. The supplementary water is supplied at a rate of 0.8 milliliters (mL) per minute.The experimental setup is shown in Fig. 1. The carbonation process was carried out with several variations in time, including a pre-

Table 1: Chemical composition of nickel slag (%, mass)

Al_2O_3	SiO_2	P_2O_5	SO_3	CaO	Cr_2O_3	MnO	FeO	NiO	CuO
0.20	8.50	0.26	0.67	0.14	0.20	0.05	75.25	0.61	0.22

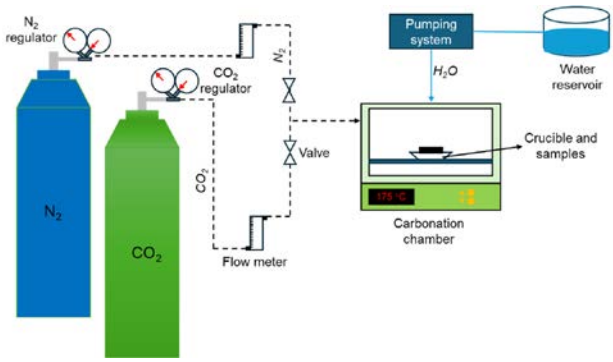


Fig. 1: The study eperimental setup

carbonation control sample, 2 hours of carbonation time (Sample A), 4 hours (Sample B), 6 hours (Sample C), 12 hours (Sample D), and 24 hours (Sample E) with temperature setting value of 200 degrees Celsius (°C). The inside temperature of carbonation chamber is about 175 °C. Following the conclusion of the process, the slag samples were removed from the oven in order to undergo additional examination through thermal gravimetric analysis (TGA) and X-ray diffraction (XRD). The TGA test was carried out to determine the CO_2 sequestration capacity. On the other hand, XRD was carried out to analyze the compounds formed during the Fe-rich slag carbonation process. For this reason, the TGA test was carried out using an N_2 atmosphere with a room temperature range of up to 1000°C. TGA heating speed is 100°C/minute (min). The TGA test was carried out at the Energy Laboratory-ITS, Surabaya, Indonesia. While XRD testing was carried out at the Department of Materials and Metallurgical Engineering-ITS, Surabaya, Indonesia using PAN Analytical equipment and CuKα radiation of 1.54056 at 2θ of 5-90°. Because iron is the dominant element contained in the Fe-rich used in this study, the calculation of $\%CO_2$ in the slag sample after the carbonation process is carried out based on the temperature range between 438-540°C. The temperature range is the decomposition temperature range of siderite ($FeCO_3$) in accordance with previous research (Luo *et al.*, 2016). The temperature of 438°C is the initial temperature of $FeCO_3$ decomposition, while the temperature of 540°C is the final temperature of the $FeCO_3$ decomposition process or reaction. Eq. 1 (Abdul *et al.*, 2023) shows the calculation for $\%CO_2$ in the slag sample after the carbonation process. Mass data at 438 and 540°C were obtained from the TGA test. On the other hand, carbonation efficiency is calculated using Eq. 2 (Wang *et al.*, 2021):

$$CO_2 \text{ in sample}(\%, \text{ mass}) = \frac{m_{438°C} - m_{540°C}}{m_{105°C}} \times 100 \quad (1)$$

$$\text{Carbonation eff.}(\%) = \frac{\text{Difference of } \%CO_2 \text{ before and after carbonation in sample}}{\text{Maximum theoretical } CO_2 \text{ content}} \times 100 \quad (2)$$

RESULTS AND DISCUSSION

CO_2 concentration in Fe-rich slag

Fig. 2(a) shows the CO_2 content in the sample both before and after the carbonation process (2-24 h) at 200 °C (Inside furnace temperature was about 175 °C), CO_2 flow of 1 L/min, N_2 flow of 4 L/min, and make-up water of 0.8 mL/min. After the carbonation process, it is evident that all samples labeled A-E or those subjected to the carbonation process for a duration of 2-24 hours exhibit the presence of CO_2. All slag samples after the carbonation process contained more CO_2 than the pre-carbonation slag samples. Prior to the carbonation process, Fe-rich slag was also known to contain CO_2. The CO_2 is believed to be produced as a result of the slag reacting with the ambient air while in storage. The subsequent section will detail the chemical reactions that could take place during the CO_2 capture process involving iron minerals in the slag. If reviewed in more detail, Sample A (carbonation process for 2 hours) has a CO_2 content of 0.99%. After 4 hours (Sample B), $\%CO_2$ in slag increased to 1.12%. Then, after 6 hours of carbonation process (Sample C), $\%CO_2$ was reduced to 0.66%. After the carbonation process ran for 12

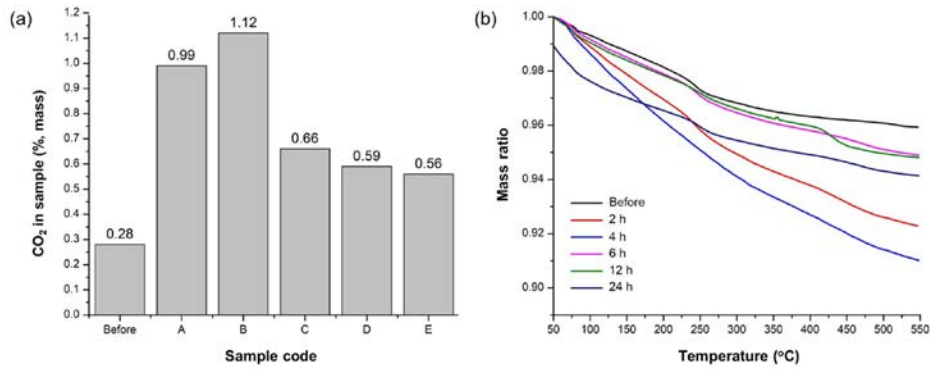


Fig. 2: (a) CO_2 in sample after carbonation process and (b) TGA plot of each sample

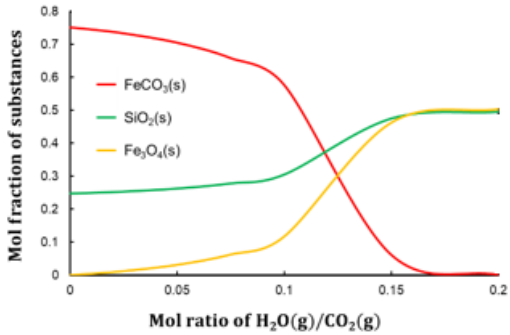


Fig. 3: Molar Ratio of $H_2O(g)$ to $CO_2(g)$ can affect the stability of $FeCO_3$. This figure was obtained using Fact-Web calculations in Equilibrium mode and without including gas products (CO_2 and H_2O) to make it easier to observe changes in $FeCO_3$, SiO_2, and Fe_3O_4.

and 24 hours, the %CO_2 in the slag sample gradually decreased to 0.59% and 0.56%. The evidence points towards a limited amount of CO_2 being captured in the surrounding area of the slag. The decrease in CO_2 after 6 hours in the sample may have been caused by the unstable bonding of iron oxide and CO_2 under experimental condition. It is highly probable that this phenomenon occurs when the process exceeds a duration of 4 hours, as observed in this study. The presence of water vapor during this extended period causes the instability of $FeCO_3$, leading to the subsequent release of CO_2. Based on calculations using Fact-Web (Bale, *et al.*, 2016), it appears that at 175 °C, $FeCO_3$ and water vapor will react to form Fe_3O_4, CO_2, and water vapor (see Fig. 3). From Fig. 3, it appears that $FeCO_3$ is increasingly unstable with more water vapor present in the system. In contrast, Fe_3O_4 tends to form more easily with more water vapor. Nonetheless, further study needs to be done to validate the results and conclusions of this preliminary study. On the other hand, Fig. 2(b) shows the mass ratio vs. temperature graph obtained from the TGA test. Based on the TGA graph, it appears that sample C (4 hours) has the most reduction in sample mass compared to other samples. Additionally, it can be inferred that the carbonation time of 4 hours yields the highest CO_2 capture rate when compared to other time frames. This is also in accordance with the calculation results shown in Fig 2(a). Typically, the low CO_2 content in slag can be attributed to the iron silicate compounds present in the slag. This condition makes the reaction between CO_2 and slag more difficult. CO_2 captured by the slag's surface indicates that iron-based compounds, including iron oxides and silicates, are involved in the capture of CO_2 gas. This is in accordance with a previous study (Hakim *et al.*, 2016) which found that iron oxide is able to capture CO_2 gas, although the role is not greater than calcium-based or magnesium-based compounds. This is because $FeCO_3$ has a lower thermodynamic stability than $CaCO_3$. $CaCO_3$ itself has a decomposition temperature of around 700°C (Karunadasa *et al.*,

2019). The temperature exceeds the decomposition temperature of $FeCO_3$, which is approximately 438°C.

Compounds and phases formed after carbonation process

To compare the XRD pattern of the Fe-rich slag sample before and after the carbonation process, XRD testing was conducted for the slag sample prior to the carbonation process, as depicted in Fig. 4. According to Fig. 4, iron silicate is the primary compound found in slag. The formation of this compound in Fe-rich slag occurs when impurities in the raw material bond together during the smelting or converting process. These bonds are formed at temperatures above the melting point of the impurities. The slag XRD graph shows that the slag has a fairly high glass phase (Liu *et al.*, 2015). The glassy phase in the slag may result from the quick cooling of Fe-rich slag in the manufacturing process. Based on XRD results, the slag sample contains three compounds, namely Fe_2SiO_4 with PDF number 96-900-0558 and Nickel iron (Ni_3Fe) with PDF number 01-088-1715. Fayalite is the dominant compound in Fe-rich slag. This is in accordance with the XRF test results which have been shown previously in Table 1. The existence of nickel iron compounds signifies the loss of nickel within the slag. Subsequent to the carbonation process, specifically after 6 hours (Sample C), iron carbonate or siderite ($FeCO_3$) in the form of carbonate compounds is detected, as indicated by PDF number 96-901-5686. The existence of iron carbonate compounds points to a chemical reaction between iron oxide and CO_2 gas resulting in $FeCO_3$ formation. Although Fe-rich slag before the carbonation process already contains CO_2 (based on Fig. 1(a), siderite peaks are still difficult to detect because of the low CO_2 content in the slag before the carbonation process. The reaction between iron oxide and CO_2 gas in producing iron carbonate is shown in Eq. 3 (Barker, *et al.*, 2018):

$$FeO(s) + CO_2(g) = FeCO_3(s) \quad (3)$$

Reynes *et al.* (2021) reported that Fe_2SiO_4 might react with CO_2 and H_2O in the wet carbonation process based on Eq. 4 (Reynes *et al.*, 2021). However, if both sides of H_2O eliminate each other, the carbonation reaction of Fe_2SiO_4 can be formulated according to Eq. 5 (Ayub *et al.*, 2020). Fig. 5 shows the thermodynamic analysis for the carbonation reaction of FeO and Fe_2SiO_4 according to Eqs. 3 and 5. Based on Fig. 5, it appears that both reactions are feasible at the experimental conditions (i.e., 175 °C).

$$Fe_2SiO_4(s) + 2CO_2(g) + 2H_2O(g) \text{ à } 2FeCO_3(s) + SiO_2(s) + 2H_2O(g) \quad (4)$$

$$Fe_2SiO_4(s) + 2CO_2(g) \text{ à } 2FeCO_3(s) + SiO_2(s) \quad (5)$$

The $FeCO_3$ peak which has a small intensity indicates that qualitatively or in general, the amount of the $FeCO_3$ compound is very small. This is in accordance with the results of the CO_2 content in Fig. 1(a). Kinetic factors seem to be the main cause for the low CO_2 capture efficiency of FeO and Fe2SiO4 in the slag under the experimental conditions of this study. Although FeO and Fe_2SiO_4 can react with CO_2

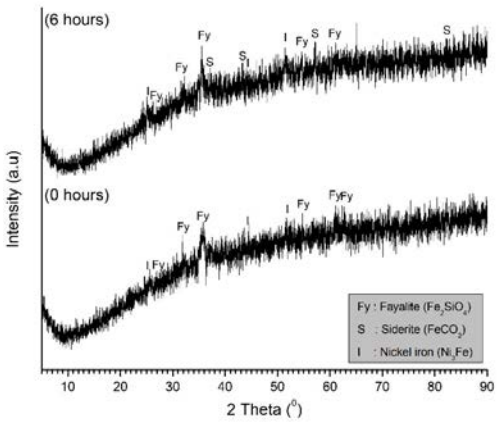


Fig. 4: Comparison between the slag sample after the carbonation process for 6 hours (Sample B) with the slag sample before the carbonation process

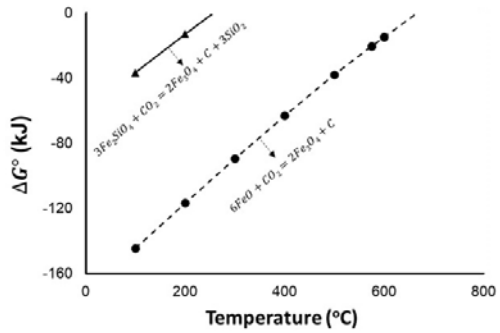


Fig. 5: Standard Gibbs energy plot as temperature increases. Thermodynamic calculations performed using Factweb (Bale, *et al.*, 2016)

thermodynamically, the reaction kinetics is very slow. The slow reaction rate is attributed to the fact that the active sites of fayalite are obstructed by a silicate structure, hindering the entry of CO_2 to these sites.

The findings of this experiment suggest that it is imperative to have a technique in place to free Fe cations from the fayalite lattice. To achieve this, pretreatment becomes necessary to release Fe cations from the silicate structure. One viable method for pretreatment is alkali fusion (Abdul, *et al.*, 2024). Consequently, the utilization of aqueous carbonation for mineral carbonation of iron minerals in Fe-rich slag is deemed superior to dry or semi-dry carbonation, based on this premise. The pretreatment process through thermal activation with alkali fusion or alkali roasting followed by washing and aqueous carbonation is an interesting option for further research.

Kinetic and possible mechanism of CO_2 capture process using Fe-rich slag

A kinetics analysis was conducted to estimate the reaction mechanism, with the assumption that the gas-solid carbonation process using Fe-rich slag followed the shrinking core model (SCM). For that, three SCM equations were used which are shown in Eqs. 6 to 8 (Wang *et al.*, 2019). Eq. 6 assumes that the carbonation reaction is controlled by mass transport. Conversely, Eqs. 7 and 8 propose that the carbonation reaction is regulated by both chemical reaction and diffusion. Where, k is the apparent reaction speed constant. α is carbonation efficiency and t is time (h).

$$kt = \alpha \tag{6}$$

$$kt = 1-(1-\alpha)^{\frac{1}{3}} \tag{7}$$

$$kt = 1-\frac{2}{3}\alpha-(1-\alpha)^{\frac{2}{3}} \tag{8}$$

Fig. 6a shows that carbonation will occur in the time range of 0-4 hours. Conversely, decarbonation occurs between 6 to 24 hours, while the kinetics analysis was conducted solely within the 0 to 4 hour timeframe. The outcomes of the kinetics analysis are detailed in Fig. 6b to d. Based on Fig. 6b to d, all models fit well with the experimental data, with R^2 values of more than 0.9 (Senthilkumaar *et al.*, 2006; Blackburne *et al.*, 2007). When the three models are compared, the diffusion model has the closest R^2 value to 1, so the rate-determining step for the CO_2 capture process by Fe-rich slag is the diffusion of CO_2 through the carbonation product layer ($FeCO_3$). With an apparent reaction rate constant value of only 3×10^{-5} /min, it appears that the gas-solid carbonation process of Fe-rich slag proceeds very slowly even though thermodynamically, the CO_2 capture process is feasible. Similar to other kinetic models, this particular model is applicable solely to Fe-rich slag with a composition specified in Table 1, and under conditions of 150 °C. Nevertheless, this study has brought forth novel findings indicating that Fe-rich slag derived from the nickel/ferronickel industry has the potential to capture CO_2 to a certain extent, a phenomenon that has not been previously reported by other researchers. Fig. 7 shows the possible mechanism of CO_2 gas binding by Fe-rich slag with a high iron oxide content. Process of capturing CO_2 by Fe-rich slag with high iron oxide content may have been caused by the reaction between FeO, Fe_2SiO_4 and CO_2 (Eqs. 3 and 5). The occurrence of

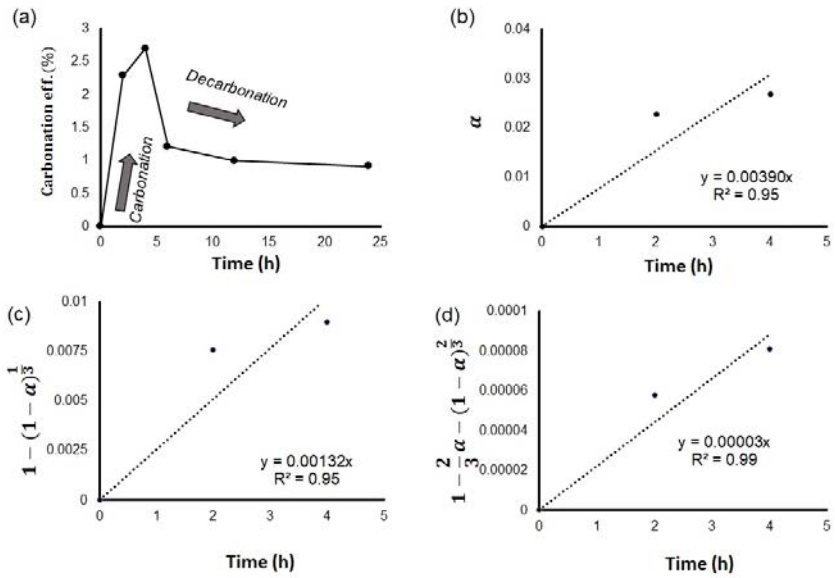


Fig. 6: (a) Carbonation efficiency plot and Analysis of Fe-rich slag carbonation reaction kinetics assuming: (a) mass transport control, (b) chemical reaction control, and (c) diffusion control

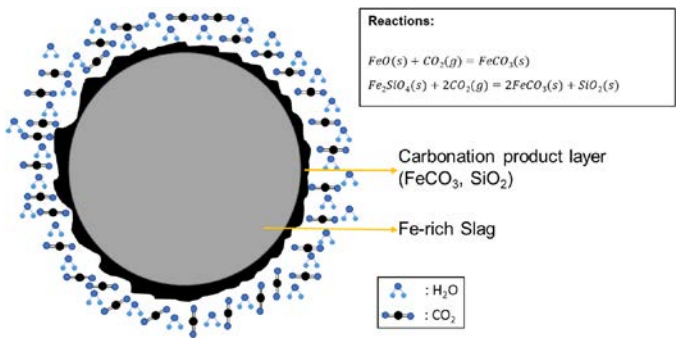


Fig. 7: Possible mechanism of CO_2 gas binding by Fe-rich slag

Table 2: Comparison of the current research with other similar studies

Year	Materials	Carbonation type	Operating parameters	CO_2 uptake (gCO_2/kg samples)	Sources
2016	Steelmaking slag (28.27% CaO, 24.25% Fe_2O_3, 15.4% SiO_2, 7.88% MgO)	Direct gas-solid	T = ambient, CO_2 = 100 vol.%, P = 10 bar	11.1	Revathy *et al.*, 2016
2018	Fly ash (28.42% CaO, 31.84% Al_2O_3, 27.67% SiO_2, 1.68% Fe_2O_3)	Direct gas-solid	T = 600 °C, 20 vol.% H_2O(g), 15 vol.% CO_2, 65 vol.% N_2 P = 1 bar	60	Liu *et al.*, 2018
2021	Red mud (27.91% Fe_2O_3, 21.91% Al_2O_3, 14.48% SiO_2, 10.65% Na_2O, 1.95% CaO)	Direct gas-solid	T = 60 °C, CO_2 = 100 vol.%, P = 45 bar	9.06	Revathy *et al.*, 2021
2024	Fe-rich slag from nickel smelter (75.25% FeO, 8.5% SiO_2, 0.14% CaO)	Direct gas-solid	T = 175 °C, CO_2 ≈ 50 vol.%, H_2O ≈ 50 vol.%, P = 1 bar	11.22	This study

carbonation on the slag's surface is facilitated by the formation of a thin interface layer, which is a result of water vapor. Both equations and water film layer produce a carbonate compound product in the form of $FeCO_3$. The carbonation reaction, specifically the formation of $FeCO_3$, is predominantly influenced by diffusion within the $FeCO_3$ product layer. Subsequently, the iron carbonate compound evolves into a passive layer, impeding the surface interaction between CO_2 gas and the fresh slag. Conversely, an excessively prolonged presence of iron-rich slag in the water vapor flow condition can lead to decarbonation, thereby reducing the efficiency of carbonation. Hence, in order to prevent decarbonation, it is essential to decrease or control the exposure of Fe-rich slag to water vapor after achieving the maximum carbonation efficiency.

Table 2 shows a comparison between the results of this study and other previous research. It appears that in terms of CO_2 uptake, Fe-rich slag in this study is comparable to red mud and steelmaking slag.

CONCLUSION

Fe-rich slag obtained form nickel smelter can be used to capture CO_2 gas by direct gas-solid mineral carbonation. The capture of CO_2 gas by the slag is due to the reaction between iron compounds (either in the form of iron oxide or iron silicate) with CO_2 gas to form siderite ($FeCO_3$) which is thermodynamically feasible at 175 °C. The CO_2 content in Fe-rich slag has been found to be higher after undergoing the carbonation process compared to its initial state. Within a 4-hours period, the $\%CO_2$ in the slag increased from 0.28% (before carbonation process) to 1.12%. The findings indicate that CO_2 capture can be achieved using Fe-rich slag. The highest carbonation efficiency value that can be achieved is only about 2.7%. The diffusion process is the key factor in controlling the CO_2 capture reaction by Fe-rich slag. Essentially, the important role is played by the diffusion of CO_2 gas into the surface layer of Fe-rich slag. During the initial 2-4 hours of carbonation, there is an observed increase in efficiency. However, after 4 hours (specifically 6 hours), the rate begins to slow due to the formation of a carbonate layer on the slag surface. As the duration of carbonation increases, efficiency decreases. The decrease may be due to the unstable $FeCO_3$ under the experimental conditions (temperature of 175 °C with CO_2 and water vapor atmosphere). CO_2 that has been mineralized in the form of $FeCO_3$ will be released back into the environment around the slag. Once the highest level of carbonation efficiency is achieved, it is crucial to swiftly convert the CO_2 and water vapor atmosphere back to the ambient air or atmosphere. This early indication highlights the necessity for prompt conversion. Thus, the CO_2 that has been mineralized in $FeCO_3$ remains stable. Despite the current low levels of CO_2 captured, the findings indicate that Fe-rich slag could be a feasible option for CO_2 capture. When Fe-rich slag from nickel smelter is blended with hot slag containing a significant amount of sensible heat, the potential for utilization becomes quite promising. In the future, it is important to carry out further research to study in more detail the potential for CO_2 gas capture using this material. Efforts to increase the reaction speed of the Fe-rich slag carbonation process need to be made in future studies. In order to address the challenges posed by the increasing positive Gibbs energy of the CO_2 capture reaction by FeO and Fe_2SiO_4 at higher temperatures, as well as the instability of $FeCO_3$ in a water vapor-rich atmosphere, it is crucial to explore the wet/aqueous carbonation method in future research. This method offers the advantage of operating at lower temperatures, usually below 90 °C, while ensuring that water remains in its liquid form instead of being in the form of gas/vapor.

AUTHOR CONTRIBUTIONS

F. Abdul as the corresponding author contributed to the experiments, data acquisition, analysis, and writing the first version of the manuscript. R.F. Rahman helped in the manuscript preparation. Y. Setiyorini contributed to reviewing the content of the manuscript. V.A. Setyowati contributed to editing and reviewing the content of the manuscript. K.A. Purwanto contributed to the experiments and data acquisition. F.I. Ma'ruf contributed to the experiments and analysis. S. Pintowantoro contributed to funding acquisition, supervising and reviewing the content of the article. All authors have reviewed the content of the article.

ACKNOWLEDGEMENT

The authors express their highest appreciation to the Ministry of Education, Culture, Research, and Higher Education-Republic of Indonesia which has supported the funding of this research through the Penelitian Tesis Magister with a research main contract number: [084/E5/PG.02.00.PT/2022] and secondary contract number [1464/PKS/ITS/2022 date: 10 May 2022].

The authors gratefully acknowledge financial support from the Institut Teknologi Sepuluh Nopember for this work, under project scheme of the Publication Writing and IPR Incentive Program (PPHKI) 2024.

CONFLICT OF INTEREST

The authors declare that there is no conflict of interests regarding the publication of this manuscript. In addition, the ethical issues, including plagiarism, informed consent, misconduct, data fabrication and/or falsification, double publication and/or submission, and redundancy have been completely observed by the authors.

OPEN ACCESS

©2024 The author(s). This article is licensed under a Creative Commons Attribution 4.0 International License, which permits use, sharing, adaptation, distribution and reproduction in any medium or format, as long as you give appropriate credit to the original author(s) and the source, provide a link to the Creative Commons license, and indicate if changes were made. The images or other third-party material in this article are included in the article's Creative Commons license, unless indicated otherwise in a credit line to the material. If material is not included in the article's Creative Commons license and your intended use is not permitted by statutory regulation or exceeds the permitted use, you will need to obtain permission directly from the copyright holder. To view a copy of this license, visit: http://creativecommons.org/licenses/by/4.0/

PUBLISHER'S NOTE

GJESM Publisher remains neutral with regard to jurisdictional claims in published maps and institutional affliations.

ABBREVIATIONS

%	Percent
°C	Degree Celcius
AISI	American iron and steel Institute
Al_2O_3	Aluminium oxide
CaO	Calcium oxide
CCS	Carbon capture and storage
CO_2	Carbon dioxide
COURSE50	CO_2 ultimate reduction system for cool earth 50
Cr_2O_3	Chromic oxide
CuO	Copper oxide
Fe	Iron
Fe_2SiO_4	Fayalite
$FeCO_3$	Siderite
FeO	Ferrous oxide
GJ	Giga joule
HYBRIT	Hydrogen breakthrough ironmaking technology
MgO	Magnesium oxide
MnO	Manganese oxide
MCC and U	Mineral carbon capture and utilization
min	Minute
mL	Milliliter
Ni_3Fe	Nickel iron
NiO	Nickel oxide
N_2	Nitrogen
NPI	Nickel pig iron
P_2O_5	Phosphorus pentoxide
RK-EF	Rotary kiln-electric furnace
SALCOS	SAlzgitter low CO_2 steelmaking
SCM	Shrinking core model
TGA	Thermal gravimatery analysis
SO_3	Sulfur trioxide
ULCOS	Ultra-low CO_2 steelmaking
XRD	X-ray diffractometer
XRF	X-ray fluroscence

REFERENCES

Abdul, F., Adachi, K., Ho, H. J., Iizuka, A., & Shibata, E. (2024). Magnesium Recovery from Ferronickel Slag by Reaction with Sodium Hydroxide. J. Environ. Chem. Eng., 12(3): 112516 **(14 pages)**.

Abdul, F.; Iizuka, A.; Ho, H.J.; Adachi, K.; Shibata, E., (2023). Potential of major by-products from non-ferrous metal industries for CO_2 emission reduction by mineral carbonation: A review. Environ. Sci. Pollut. Res., 30: 78041–78074 **(34 pages)**.

Ayub, S.A.; Tsegab, H.; Rahmani, O.; Beiranvand P.A., (2020). Potential for CO_2 mineral carbonation in the paleogene segamat basalt of Malaysia. Minerals. 10(12): 1045 **(14 pages)**.

Bale, C.W.; Bélisle, E.; Chartrand, P.; Decterov, S.A.; Eriksson, G.; Gheribi, A.E.; Hack, K.; Jung, I-H.; Kang, Y-B.; Melancon, J.; Pelton, A.D.; Petersen, S.; Robelin, C.; Sangster, J.; Spencer, P; Van Ende, M.A. (2016). Reprint of: FactSage thermochemical software and databases, 2010–2016. Calphad. 55: 1-19 **(19 pages)**.

Barker, R.; Burkle, D.; Charpentier, T.; Thompson, H.; Neville, A., (2018). A review of iron carbonate ($FeCO_3$) formation in the oil and gas industry. Corros. Sci., 142: 312-341 **(30 pages)**.

Blackburne, R.; Vadivelu, V.M.; Yuan, Z.; Keller, J., (2007). Kinetic characterisation of an enriched Nitrospira culture with comparison

to Nitrobacter. Water Res., 41(14): 3033-3042 **(10 pages)**.

Chen, Z.; Cang, Z.; Yang, F.; Zhang, J.; Zhang, L., (2021). Carbonation of steelmaking slag presents an opportunity for carbon neutral: A review. J. CO_2 Util., 54: 101738 **(14 pages).**

Gao, F.; Huang, Z.; Li, H.; Li, X.; Wang, K.; Hamza, M.F.; Wei, Y.; Fujita, T., (2021). Recovery of magnesium from ferronickel slag to prepare hydrated magnesium sulfate by hydrometallurgy method. J. Clean. Prod., 303: 127049 **(12 pages)**.

Hakim, A.; Marliza, T.S.; Abu T.N.M.; Wan I.R.W.; Yusop, R.M.; Mohamed H.W.M.; Yarmo, A.M., (2016). Studies on CO_2 adsorption and desorption properties from various types of iron oxides (FeO, Fe_2O_3, and Fe_3O_4). Ind. Eng. Chem. Res., 55(29): 7888-7897 **(10 pages)**.

Han, C.; Hong, Y.C., (2018). Adverse health effects of ferronickel manufacturing factory on local residents: An interrupted time series analysis. Environ. Int., 114: 288-296 **(9 pages)**.

Hassan, S.T; Xia, E.; Lee, C.C., (2021). Mitigation pathways impact of climate change and improving sustainable development: The roles of natural resources, income, and CO_2 emission. Energy Environ., 32(2): 338-363 **(6 pages)**.

Ho, H.J.; Iizuka, A.; Shibata, E.; Tomita, H.; Takano, K.; Endo, T., (2020). CO_2 utilization via direct aqueous carbonation of synthesized concrete fines under atmospheric pressure. ACS Omega. 5(26): 15877-15890 **(14 pages).**

Ho, H.J.; Iizuka, A.; Shibata, E., (2021a). Utilization of low-calcium fly ash via direct aqueous carbonation with a low-energy input: Determination of carbonation reaction and evaluation of the potential for CO_2 sequestration and utilization. J. Environ. Manage., 288: 112411 **(11 pages).**

Ho, H.J; Iizuka, A.; Shibata, E.; Tomita, H.; Takano, K.; Endo, T., (2021b). Utilization of CO_2 in direct aqueous carbonation of concrete fines generated from aggregate recycling: Influences of the solid–liquid ratio and CO_2 concentration. J. Cleaner Prod., 312, 127832 **(10 pages).**

Iizuka, A.; Sasaki, T.; Honma, M.; Yoshida, H.; Hayakawa, Y.; Yanagisawa, Y.; Yamasaki, A., (2017). Pilot-scale operation of a concrete sludge recycling plant and simultaneous production of calcium carbonate. Chem. Eng. Commun., 204(1): 79-85 **(7 pages).**

Karunadasa, K.S.; Manoratne, C.H.; Pitawala, H.M.T.G.A.; Rajapakse, R.M.G., (2019). Thermal decomposition of calcium carbonate (calcite polymorph) as examined by in-situ high-temperature X-ray powder diffraction. J. Phys. Chem. Solids. 134: 21-28 **(8 pages)**.

Kasikov, A.G.; Shchelokova, E.A.; Timoshchik, O.A.; Sokolov, A.Y., (2022). Utilization of converter slag from nickel production by hydrometallurgical method. Metals, 12(11): 1934 **(14 pages).**

Kuri, J.C.; Majhi, S.; Sarker, P.K.; Mukherjee, A., (2021). Microstructural and non-destructive investigation of the effect of high temperature exposure on ground ferronickel slag blended fly ash geopolymer mortars. J. Build. Eng., 43: 103099 **(14 pages)**.

Kuri, J.C.; Nuruzzaman, M.; Sarker, P.K., (2022). Sodium sulphate resistance of geopolymer mortar produced using ground ferronickel slag with fly ash. Ceram. Int., 49(2): 2765-2773 **(9 pages)**.

Li, J.; Sun, Z.; Wang, L.; Yang, X.; Zhang, D.; Zhang, X.; Wang, M., (2022). Properties and mechanism of high-magnesium nickel slag-fly ash based geopolymer activated by phosphoric acid. Constr. Build. Mater., 345: 128256 **(14 pages)**.

Liu, J.; Yu, Q.; Duan, W.; Qin, Q., (2015). Experimental investigation of glass content of blast furnace slag by dry granulation. Environ. Prog. Sustainable Energy. 34(2): 485-491 **(7 pages)**.

Liu, S.; Li, H.; Zhang, K.; Lau, H.C., (2022). Techno-economic analysis of using carbon capture and storage (CCS) in decarbonizing China's coal-fired power plants. J. Cleaner Prod., 351: 131384 **(8 pages).**

Liu, W.; Su, S.; Xu, K.; Chen, Q.; Xu, J.; Sun, Z.; Wang, Y.; Hu, S.; Wang, X.; Xue, Y.; Xiang, J., (2018). CO_2 sequestration by direct gas–solid carbonation of fly ash with steam addition. J. Clean. Prod., 178: 98-107 **(10 pages)**.

Liu, W.; Zuo, H.; Wang, J.; Xue, Q.; Ren, B.; Yang, F., (2021). The production and application of hydrogen in steel industry. Int. J. Hydrogen Energy. 46(17): 10548-10569 **(22 pages).**

Luo, Y.H.; Zhu, D.Q.; Pan, J.; Zhou, X.L., (2016), Thermal decomposition behaviour and kinetics of Xinjiang siderite ore. Miner. Process. Extr. Metal., 125(1): 17-25 **(9 pages)**.

Mistry, M.; Gediga, J.; Boonzaier, S., (2016). Life cycle assessment of nickel products. The International Journal of Life Cycle Assessment, 21: 1559-1572 **(14 pages)**.

Nuruzzaman, M.; Kuri, J.C.; Sarker, P.K., (2022). Strength, permeability and microstructure of self-compacting concrete with the dual use of ferronickel slag as fine aggregate and supplementary binder. Constr. Build. Mater., 318: 125927 **(12 pages)**.

Pintowantoro, S.; Panggabean, P.C.; Setiyorini, Y.; Abdul, F., (2022). Smelting and selective reduction of limonitic laterite ore in mini blast furnace. J. Inst. Eng. India Ser. D., 103(2): 591-600 **(10 pages)**.

Pintowantoro, S.; Pasha, R.A.M.; Abdul, F., (2021). Gypsum utilization on selective reduction of limonitic laterite nickel. Results Eng., 12: 100296 **(8 pages)**.

Revathy, T.D.R.; Palanivelu, K.; Ramachandran, A., (2016). Direct mineral carbonation of steelmaking slag for CO_2 sequestration at room temperature. Environ. Sci. Pollut. Res., 23: 7349-7359 **(11 pages)**.

Revathy, T.D.R.; Ramachandran, A.; Palanivelu, K., (2021). Sequestration of CO_2 by red mud with flue gas using response surface methodology. Carbon Manage., 12(2): 139-151 **(13 pages)**.

Reynes J.F.; Mercier G.; Blais J.F.; Pasquier L.C., (2021). Feasibility of a mineral carbonation technique using iron-silicate mining waste by direct flue gas CO_2 capture and cation complexation using 2,2'-bipyridine. Minerals. 11(4):343 **(19 pages)**.

Senthilkumaar, S.; Kalaamani, P.; Subburaam, C.V., (2006). Liquid phase adsorption of crystal violet onto activated carbons derived from male flowers of coconut tree. J. Hazard. Mater., 136(3): 800-808 **(9 pages)**.

Shang, W.; Peng, Z.; Xu, F.; Tang, H.; Rao, M.; Li, G.; Jiang, T., (2021). Preparation of enstatite-spinel based glass-ceramics by co-utilization of ferronickel slag and coal fly ash. Ceram. Int., 47(20): 29400-29409 **(10 pages)**.

Sun, W.; Wang, Q.; Zhou, Y.; Wu, J., (2020). Material and energy flows of the iron and steel industry: Status quo, challenges and perspectives. Appl. Energy. 268: 114946 **(15 pages).**

Sun, Y.; Tian, S.; Ciais, P.; Meng, J.; Zhang, Z., (2022) Decarbonising the iron and steel sector for a 2 °C target using inherent waste streams. Nat. Commun., 13: 297 **(8 pages).**

Tang, H.; Peng, Z.; Shang, W.; Ye, L.; Luo, J.; Rao, M.; Li, G., (2022). Preparation of refractory materials from electric furnace ferronickel slag and blast furnace ferronickel slag: A comparison. J. Environ. Chem. Eng., 10(3): 107929 **(11 pages)**.

Wang, F.; Dreisinger, D.; Jarvis, M.; Hitchins, T., (2019). Kinetics and mechanism of mineral carbonation of olivine for CO_2 sequestration. Miner. Eng., 131: 185-197 **(13 pages)**.

Wang, F.; Dreisinger, D.; Jarvis, M.; Hitchins, T., (2021). Kinetic evaluation of mineral carbonation of natural silicate samples. Chem. Eng. J., 404: 126522 **(9 pages).**

Wang, Y.; Zhu, R.; Chen, Q.; Wei, G.; Hu, S.; Guo, Y., (2018). Recovery of Fe, Ni, Co, and Cu from nickel converter slag through oxidation and reduction. ISIJ Int., 58(12): 2191-2199 **(9 pages)**.

Wei W.; Samuelsson, P.B.; Tilliander A.; Gyllenram R.; Jönsson P.G., (2020). Energy Consumption and Greenhouse Gas Emissions of Nickel Products. Energies. 13(21): 5664 **(22 pages)**.

Widyartha, B.; Setiyorini, Y.; Abdul, F.; Subakti, T.J..; Pintowantoro,

S., (2020). Effective beneficiation of low content nickel ferrous laterite using fluxing agent through Na2SO4 selective reduction. Materialwiss. Werkstofftech. 51(6): 750-757 **(8 pages).**

World Steel Association, (2023). Sustainability indicator report **(9 pages)**

Wu, X.; Gu, F.; Su, C.; Wang, W.; Pu, K.; Shen, D.; Long, Y., (2022). Preparing high-strength ceramsite from ferronickel slag and municipal solid waste incineration fly ash. Ceram. Int., 48(23): 34265-34272 **(8 pages)**.

Zulhan, Z.; Agustina, N., (2021). A novel utilization of ferronickel slag as a source of magnesium metal and ferroalloy production. J. Clean. Prod., 292: 125307 **(13 pages)**.

AUTHOR (S) BIOSKETCHES

Abdul, F., M.T., Assistant Professor, Department of Materials and Metallurgical Engineering, Faculty of Industrial Technology and System Engineering, Institut Teknologi Sepuluh Nopember, Arief Rahman Hakim Street, Surabaya, 60111, Indonesia
- Email: *fakhrezaabdul@gmail.com*
- ORCID: 0000-0003-1048-0717
- Web of Science ResearcherID: CAG-2214-2022
- Scopus Author ID: 57201672383
- Homepage: https://scholar.its.ac.id/en/persons/fakhreza-abdul

Rahman, R.F., M.T., former student, Department of Materials and Metallurgical Engineering, Faculty of Industrial Technology and System Engineering, Institut Teknologi Sepuluh Nopember, Arief Rahman Hakim Street, Surabaya, 60111, Indonesia.
- Email: *raisfrahman@gmail.com*
- ORCID: 0009-0000-5403-6154
- Web of Science ResearcherID: NA
- Scopus Author ID: NA
- Homepage: https://repository.its.ac.id/104698/

Purwanto, K.A., S.T., former student, Department of Materials and Metallurgical Engineering, Faculty of Industrial Technology and System Engineering, Institut Teknologi Sepuluh Nopember, Arief Rahman Hakim Street, Surabaya, 60111, Indonesia.
- Email: *kaisarakbar14@gmail.com*
- ORCID: 0009-0000-2635-3304
- Web of Science ResearcherID: NA
- Scopus Author ID: NA
- Homepage: https://www.its.ac.id/tmaterial/id/alumni/daftar-alumni/

Ma'ruf, F.I., S.T., former student, Department of Materials and Metallurgical Engineering, Faculty of Industrial Technology and System Engineering, Institut Teknologi Sepuluh Nopember, Arief Rahman Hakim Street, Surabaya, 60111, Indonesia.
- Email: *fazafiizzul@gmail.com*
- ORCID: 0009-0009-4806-9852
- Web of Science ResearcherID: NA
- Scopus Author ID: NA
- Homepage: https://www.its.ac.id/tmaterial/id/alumni/daftar-alumni/

Setiyorini, Y., Ph.D, Assistant Professor, Department of Materials and Metallurgical Engineering, Faculty of Industrial Technology and System Engineering, Institut Teknologi Sepuluh Nopember, Arief Rahman Hakim Street, Surabaya, 60111, Indonesia.
- Email: *yuli_setyo@mat-eng.its.ac.id*
- ORCID: 0000-0002-9566-4701
- Web of Science ResearcherID: FWO-8384-2022
- Scopus Author ID: NA
- Homepage: https://scholar.its.ac.id/en/persons/yuli-setiyorini

Setyowati, V.A., M.T., Assistant Professor, Department of Mechanical Engineering, Faculty of Industrial Technology, Institut Teknologi Adhi Tama Surabaya, Arief Rahman Hakim Street, Surabaya, 60117, Indonesia
- Email: *vuri@itats.ac.id*
- ORCID: 0000-0003-3520-7821
- Web of Science ResearcherID: CAI-0588-2022
- Scopus Author ID: 55873007300
- Homepage: https://me.itats.ac.id/vuri/

Pintowantoro, S., Ph.D., Professor, Department of Materials and Metallurgical Engineering, Faculty of Industrial Technology and System Engineering, Institut Teknologi Sepuluh Nopember, Arief Rahman Hakim Street, Surabaya, 60111, Indonesia.
- Email: *sungging@mat-eng.its.ac.id*
- ORCID: 0000-0002-2615-2657
- Web of Science ResearcherID: CAG-3004-2022
- Scopus Author ID: 6507392773
- Homepage: https://scholar.its.ac.id/en/persons/sungging-pintowantoro

HOW TO CITE THIS ARTICLE

Abdul, F.; Rahman, F.; Purwanto, K.A.; Ma'ruf, F.I.; Setiyorini, Y.; Setyowati, V.A.; Pintowantoro, S., (2024). Application of iron-rich slag to capture carbón dioxide gas through direct gas-solid carbonation. Global J. Environ. Sci. Manage., 10(4): 1675-1686.

DOI: 10.22034/gjesm.2024.04.11

URL: https://www.gjesm.net/article_712299.html